

## Article

# Geochemical Characteristics of Nephrite from Chuncheon, South Korea: Implications for Geographic Origin Determination of Nephrite from Dolomite-Related Deposits

Nan Li, Feng Bai \*, Qi Peng and Mengsong Liu

School of Gemology, China University of Geosciences (Beijing), No. 29 Xueyuan Road, Haidian District, Beijing 100083, China; linan69@foxmail.com (N.L.); 15614410272@163.com (Q.P.); 15901050539@163.com (M.L.)

\* Correspondence: baifeng@cugb.edu.cn

**Abstract:** The Chuncheon nephrite deposit in South Korea is one of the major nephrite deposits in the world, but its origin has been rarely studied. This study explores the mineralogical and geochemical characteristics of the Chuncheon nephrite using a polarizing microscope, an electron microprobe, laser ablation, inductively coupled plasma mass spectrometry, and hydrogen–oxygen isotope analyses and compares them with dolomite-related nephrite worldwide. The main mineral of Chuncheon nephrite is tremolite, which has a felted blastic texture, secondary filling texture, and metasomatic pseudomorphic texture that nephrites from other regions do not have. Chuncheon nephrite is dolomite-related; the total content of rare earth elements is generally low, with highly variable positive and negative Eu anomalies and weak positive Ce anomalies; and the light rare earth elements are enriched. The Chuncheon nephrite formed in an anaerobic alkaline environment with a low degree of mineralization, and the hydrothermal fluids are predominantly meteoric water. Nephrite from different regions has different geochemical characteristics as well as different abundances of rare earth element contents. According to the content and range of elements, such as  $\delta\text{Ce}$ ,  $\delta\text{Eu}$ ,  $\Sigma\text{REE}$ ,  $(\text{La}/\text{Sm})\text{N}$ , and other rare earth elements, dolomite-type nephrite from different origins can be roughly distinguished.



**Citation:** Li, N.; Bai, F.; Peng, Q.; Liu, M. Geochemical Characteristics of Nephrite from Chuncheon, South Korea: Implications for Geographic Origin Determination of Nephrite from Dolomite-Related Deposits. *Crystals* **2023**, *13*, 1468. <https://doi.org/10.3390/crust13101468>

Academic Editor: Vladislav V. Gurzhiy

Received: 12 September 2023

Revised: 30 September 2023

Accepted: 2 October 2023

Published: 8 October 2023



**Copyright:** © 2023 by the authors. Licensee MDPI, Basel, Switzerland. This article is an open access article distributed under the terms and conditions of the Creative Commons Attribution (CC BY) license (<https://creativecommons.org/licenses/by/4.0/>).

**Keywords:** geochemistry; Chuncheon nephrite; dolomite-related nephrite; origins characteristics

## 1. Introduction

Nephrite is a mineral aggregate that is mainly composed of tremolite and actinolite, and it has an important position in the world of non-metallic minerals. Nephrite deposits are widely distributed worldwide in several countries, such as Russia [1–3], Poland [4,5], Italy [6], Canada [7–10], Australia [11,12], South Korea [13–26], and China [24–46]. The nephrite deposit is located in the east of Chuncheon, South Korea, and is one of the largest nephrite deposits in the world. Nephrite deposit types can be classified as dolomite- or serpentine-related according to their genesis [10,47]. Dolomite-related nephrite mainly forms in the contact zone between dolomite and magmatic rock. The intrusive rocks of dolomite-related nephrite deposits are acidic magmatic rocks, such as in Russia [1,3], Canada [8,10], and Heilongjiang, China [45]; moderately acidic magmatic rocks, such as in Liaoning, China [7,35,36] and Xingjiang, China [39–41]; and basal magmatic rocks, such as in Guangxi, China [27–29,46] and Guizhou, China [31–33]. The formation of the Chuncheon nephrite deposit is mainly associated with dolomitic marble, but different theories have been proposed for the mineralization mechanisms. Some researchers believe that acidic granites provide necessary materials for the formation of nephrite [15,20,33], while others believe that biotite schist provides necessary materials [19]. The texture [18,22], composition [15,16,20,24], gemological characteristics [18,20–22,25], and stable isotopes [14,17] of the Chuncheon nephrite have been previously studied, but the geographic origin characteristics of the Chuncheon nephrite have not been comprehensively studied. Herein,

we systematically analyze the geochemical characteristics of the Chuncheon nephrite and compare them with those of the dolomite-related nephrite of other geographic origins. This is conducted to distinguish the geochemistry characteristics of the Chuncheon nephrite and provide evidence of its genesis.

## 2. Geological Setting

The Yonduri gneiss complex mainly comprises biotite schists, banded biotite gneisses, and muscovite gneisses, which crop out in the mine area immediately below the metasedimentary rocks of the Gubongsan Group that overlies the Yonduri gneiss complex [13]. Augen gneisses and porphyritic orthogneisses are usually found in the contact zone between the biotite schists, and a granitic gneiss of unknown age lies to the east of the mine area. To the south of the biotite schists, the Gubongsan Group, from the north to the south, comprises a lower amphibolite of the Pyeongchonri Formation and the Shiniri Formation and an upper amphibolite of the Gamjeongri Formation (Figure 1).

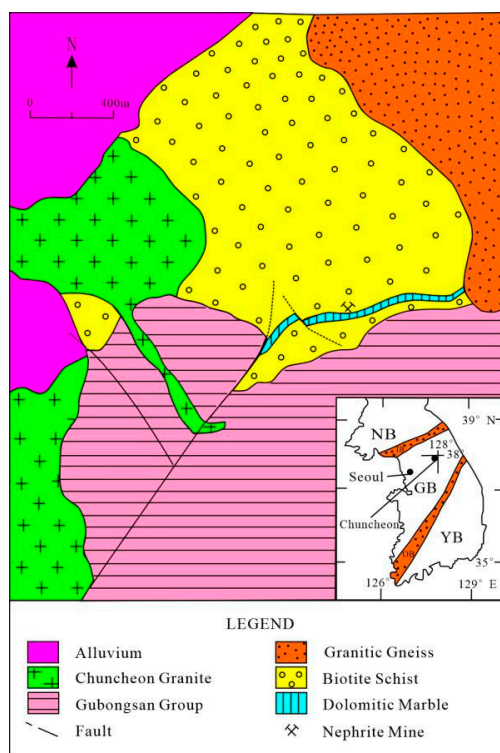


**Figure 1.** Simplified geologic map of the region and location of the Chuncheon nephrite deposit (adapted from Yui and Kwon, 2002) [17].

Both the Yonduri Gneiss Group and the Gubongsan Group are intruded by the mesozoic Chuncheon granite and cut off by the northeast–southwest fault to the west. Furthermore, there is no direct contact between the granite and nephrite deposits. Chuncheon granite is a biotite granite that forms two extensive areas to the northwest and southwest of the mine area; however, immediately to the west of the mine, the granite crops out as an unusual vein-like body [13] (Figure 2).

Based on the Th–U–Pb age dating of monazite, the metamorphic age of the northern part of the Gyeonggi Block (located ~30 km northwest of the Chuncheon nephrite mine) is Triassic ( $245 \pm 3$  Ma) [23], when the Nangrim and Gyeonggi blocks collided. The K–Ar dating of the Chuncheon granite also suggests a Late Triassic intrusion age of  $210.5 \pm 5.0$  Ma and a cooling age of 170 Ma below the Early Jurassic age of  $300^{\circ}\text{C}$  [13]. These age data confirm that the Chuncheon granite formed post-tectonically.

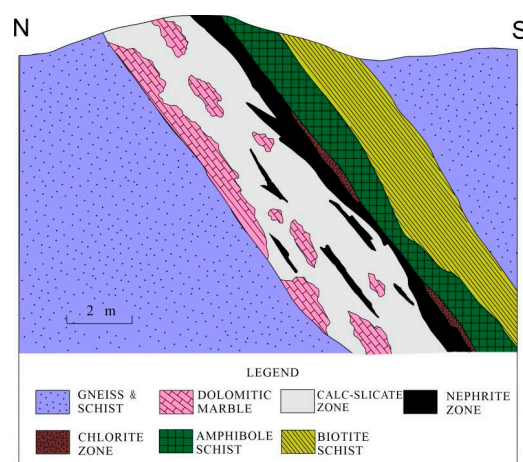


**Figure 2.** Schematic cross section of the Chuncheon nephrite deposit (adapted from Yui and Kwon, 2002) [17].

The nephrite belt and surrounding rocks are buried in the order (from bottom to top) of light gneiss, white mafic barite, calcite silicate belt, nephrite belt, chlorite belt, hornblende schist belt, biotite schist belt, and light gneiss (Figure 2). The nephrite occurs as lenses that are generally several meters long and up to 1 m thick. The lithologic contacts and the major schistosity trend are mainly east–west, with dips of 35°–50° toward the south [13,17].

### 3. Samples and Methods

#### 3.1. Samples

In this study, four representative Chuncheon nephrite samples are collected, namely, KC-1–KC-4, according to their color (Figure 3). KC-1 has a cyan color with a coarse texture; KC-2 has a greenish-white color with a transition from cyan to white; KC-3 has a white color with a more delicate texture and dark dotted inclusions that are locally visible; and the color of KC-4 transitions from yellow-white to dark brown, and the deep yellow-brown graininess is strong.

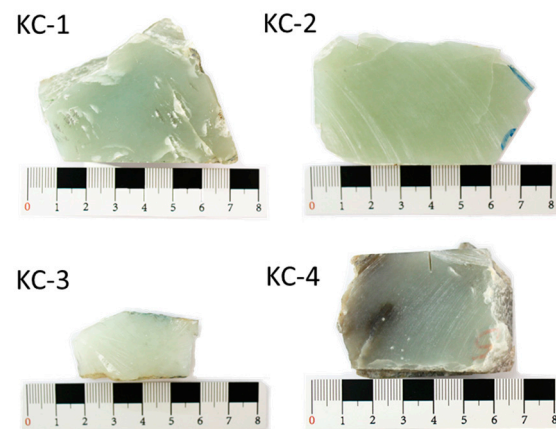


**Figure 3.** Pictures of hand specimens of nephrite from the Chuncheon deposit.

#### 3.2. Methods

The samples were cut into thin sections (0.03 mm thick) and were later powdered up to 300 mesh in a grinding chamber at the China University of Geosciences (Beijing). The sheets were observed under a polarized microscope (BX5, Olympus, Tokyo, Japan).

An electron probe microanalysis (EPMA) experiment and back-scattered electron observations were conducted in the Electron Probe and Scanning Electron Microscope Laboratory of the Institute of Geology and Geophysics, Chinese Academy of Sciences (CAS;

JXA-8100 electron probe, JEOL Ltd., Tokyo, Japan). Ten microzone elements were analyzed, with a beam spot diameter of 5  $\mu\text{m}$ , a beam current of 20 nA, and an accelerating voltage of 15 kV.

A laser ablation inductively coupled plasma mass spectrometry (LA-ICP-MS) analysis was performed in the Inductively Coupled Ion Mass Spectrometry Laboratory at the Institute of Geology and Geophysics, CAS (Q-ICP-MS model 7500a, Agilent, Santa Clara, CA, USA). The laser wavelength and diameter were 193 nm and 60  $\mu\text{m}$ , respectively, and the erosion frequency was 80 Hz.

The hydrogen–oxygen stable isotope analysis was performed at the Analysis and Testing Research Center of the Beijing Research Institute of Nuclear Industry. The samples were analyzed by the conventional  $\text{BrF}_5$  method for their oxygen isotope compositions [48]. The precision of the analyses was generally better than  $\pm 0.2$  per mil. The results are reported as  $\delta^{18}\text{O}$  values relative to V-SMOW. Hydrogen isotope analyses on hydrous minerals were performed after the method of Godfrey with a precision of  $\pm 2$  per mil [49]. The results are reported as  $\delta\text{D}$  values relative to V-SMOW. A MAT-253 mass spectrometer was used to measure the isotope compositions.

#### 4. Results

##### 4.1. Mineralogical Characteristics

The samples mainly comprise tremolite, which exhibits a second-level, blue-green-purple interference color under cross-polarized light (Figure 4a,b). Tremolite has a microscopically fibrous and interwoven appearance, and the texture is mainly a felt-like fibroblastic texture (Figure 4c,d). The long diameter of the grain size is below 0.02 mm, which is an important reason for the fine and moist texture of nephrite.

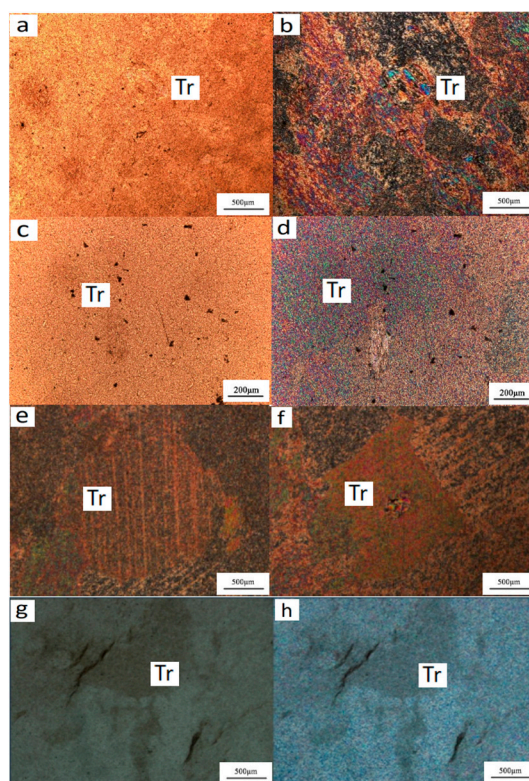


**Figure 4.** Microtexture of the Chuncheon nephrite. (a–d) Tremolite has a felt-like fibroblastic texture. (e,f) early calcite or dolomite particles replaced by late tremolite (based on the pseudomorphic metasomatic texture). (g,h) microfractures in nephrite filled with iron impurities. Tr: tremolite.

In the pseudomorphic metasomatic texture of the Chuncheon nephrite (Figure 4e,f), with KC-4 exhibiting the most texture, calcite or dolomite particles are accounted for by

tremolite, preserving the morphology and cleavage of the carbonate mineral. This metasomatic replacement texture is widespread in the Chuncheon nephrite samples, indicating that the Chuncheon nephrite underwent only weak recrystallization in the later stages and that the geographic origin of the texture is relatively inhomogeneous [19]. This type of texture is not common in dolomite-related deposits of nephrite of other geographic origins.

In KC-4, the crystal particles are larger and have a rougher texture compared to the other samples. Yellowish-brown iron impurities can be observed in the interstices of microfractures and pseudomorphic grain in the nephrite (Figure 4g); this secondary filling texture indicates different degrees of structural denseness of the Chuncheon nephrite.

#### 4.2. Electron Microprobe Analysis

The average contents of  $\text{SiO}_2$ ,  $\text{MgO}$ ,  $\text{CaO}$ , and  $\text{FeO}$  in the samples are 58.98, 23.97, 12.47, and 0.34 wt%, respectively (Table 1), which are close to the theoretical values of the tremolite mineral composition ( $\text{SiO}_2$ : 59.169 wt%;  $\text{MgO}$ : 24.808 wt%;  $\text{CaO}$ : 13.805 wt%) and exhibit high Mg and Si content and low Fe and Ca content characteristics.

The official International Mineralogical Association (IMA) formulas for tremolite and actinolite are  $\text{Ca}_2(\text{Mg}_{5.0-4.5}\text{Fe}^{2+}_{0.0-0.5})\text{Si}_8\text{O}_{22}(\text{OH})_2$  and  $\text{Ca}_2(\text{Mg}_{4.5-2.5}\text{Fe}^{2+}_{0.5-2.5})\text{Si}_8\text{O}_{22}(\text{OH})_2$ , respectively. In these formulas,  $\text{Mg}^{2+}$  and  $\text{Fe}^{2+}$  can be substituted via complete isomerization. According to the hornblende nomenclature of IMA, the naming decision is based on the occupancy unit texture of  $\text{Mg}^{2+}$  and  $\text{Fe}^{2+}$  within the region. For tremolite, actinolite, and ferroactinolite,  $\text{Mg}^{2+}/(\text{Mg}^{2+} + \text{Fe}^{2+}) = 0.90-1.00$ , 0.50–0.90, and 0.00–0.50, respectively. The respective cation and  $\text{Fe}^{2+}/\text{Fe}^{3+}$  coefficients were obtained by calculating the chemical formulas based on the 23 oxygen ions according to the IMA hornblende naming rules.

The calculation of the  $\text{Mg}^{2+}/(\text{Mg}^{2+} + \text{Fe}^{2+})$  values and Si cation number in the 36 groups of the hornblende minerals shows that all samples belong to tremolite and that all  $\text{Mg}^{2+}/(\text{Mg}^{2+} + \text{Fe}^{2+})$  values are greater than 0.99, indicating that the tremolite mineral composition has a very low Fe content (0.22–0.55 wt%). Hence, the samples exhibit the characteristics of high Mg content and low Fe content (Table 1).

The average values of  $\text{FeO}$  in the white nephrite, green-white nephrite, and green nephrite were 0.258, 0.335, and 0.470 wt%, respectively. The  $\text{FeO}$  content increased as the color deepened, and  $\text{FeO}$  was associated with the green of the samples. According to the electron microprobe results and mineral chemical formula electrovalent balance, it is calculated that all the Fe in the samples is  $\text{Fe}^{2+}$ .

#### 4.3. LA-ICP-MS Analysis

Table 2 lists the mass fractions of the trace elements and rare earth elements (REEs) in the nephrite samples. The sample REE and trace elemental contents were normalized using the Boynton chondrite [50] and McDonough primitive mantle element concentrations [51]. Most elements are measured to an accuracy of 0.001, and some elements, such as Cr, Ni, Zn, and Sr, are measured to an accuracy of 0.01.

LA-ICP-MS analysis showed that the samples had low contents of REEs ( $\Sigma\text{REE} = 1.507-2.731$  ppm) and light REEs (LREEs; 1.278–2.373 ppm). The content of heavy REEs (HREEs) was low (0.229–0.400 ppm). The LREE/HREE range was 4.13–9.04, indicating that LREEs are more abundantly present than HREEs.  $\delta\text{Eu}$  (0.11–3.53) exhibits both positive and negative anomalies, and the degree of anomalies is highly variable.  $\delta\text{Ce}$  (1.31–1.63) exhibits a weak positive anomaly.  $\text{La}_N/\text{Sm}_N$ ,  $\text{Sm}_N/\text{Ho}_N$ , and  $\text{Gd}_N/\text{Lu}_N$  are used to indicate the degree of differentiation of the light, medium, and heavy REEs of the samples. The high  $\text{La}_N/\text{Sm}_N$  values (1.96–48.79) of the Chuncheon nephrite indicate a significantly higher degree of LREE differentiation, the large  $\text{Sm}_N/\text{Ho}_N$  differences (0.09–4.00) indicate a large difference in the degree of medium rare earth element differentiation, and the  $\text{Gd}_N/\text{Lu}_N$  values (0.10–2.99) indicate a low degree of HREE differentiation.





Rb, and the high field strength elements Nb, Zr, Hf, and Y are generally depleted. Overall, the trace elemental content is very low.

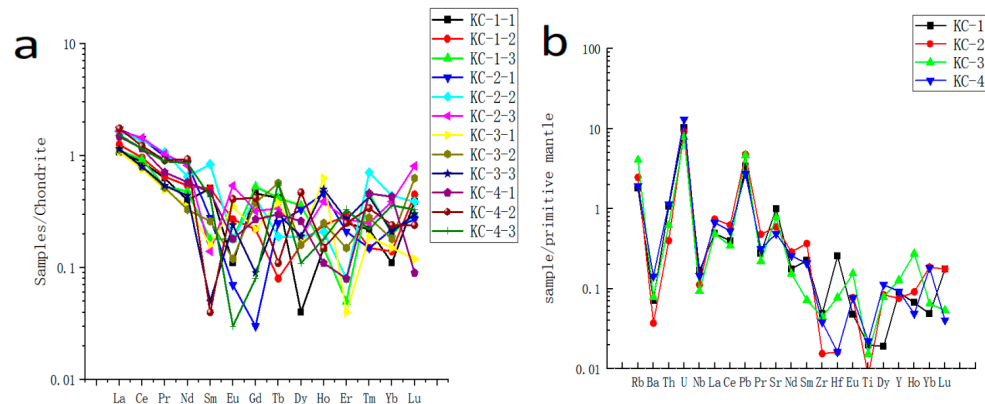


**Figure 5.** (a) Chondrite-normalized REE patterns of selected samples. (b) Primitive mantle-normalized trace element diagrams of selected samples.

The Ni content of the Chuncheon nephrite samples ranges from 9.1 to 16.7 ppm, with samples KC-3, KC-2, and KC-1 showing a color transition from white to cyan, with the Ni content increasing when the color turns to cyan.

#### 4.4. Hydrogen–Oxygen Isotope Analysis

The  $\delta^{18}\text{O}$  and  $\delta\text{D}$  ranges of the samples are respectively  $-7.2\text{\textperthousand}$  to  $-2.9\text{\textperthousand}$  and  $-117\text{\textperthousand}$  to  $-109\text{\textperthousand}$  (Table 3). Tremolite formation is insensitive to changes in  $\delta\text{D}$  values when the temperature ranges from  $350\text{ }^{\circ}\text{C}$  to  $650\text{ }^{\circ}\text{C}$  [52]. Assuming that tremolite in the samples is formed at a temperature range from  $330\text{ }^{\circ}\text{C}$  to  $450\text{ }^{\circ}\text{C}$ , the oxygen isotopic composition of the hydrothermal fluids at  $330\text{ }^{\circ}\text{C}$ ,  $390\text{ }^{\circ}\text{C}$ , and  $450\text{ }^{\circ}\text{C}$  can be calculated based on the fractionation equation  $10^3\ln\alpha = 3.95 \times 10^6/T^2 - 8.28 \times 10^3/T + 2.38$  [53]. The  $\delta\text{D}$  composition (Table 3) of the hydrothermal fluids was calculated using the tremolite–water fraction geothermometer proposed by Graham et al. (1984) by setting  $\delta\text{D}$  tremolite–water =  $-21.7\text{\textperthousand}$  and the temperature range to  $330\text{ }^{\circ}\text{C}$ – $450\text{ }^{\circ}\text{C}$ . The  $\delta^{18}\text{O}$  and  $\delta\text{D}$  isotopic results correspond to  $\delta^{18}\text{O} = -6.7\text{\textperthousand}$ – $-2.4\text{\textperthousand}$  ( $330\text{ }^{\circ}\text{C}$ ),  $-6.1\text{\textperthousand}$ – $-1.8\text{\textperthousand}$  ( $390\text{ }^{\circ}\text{C}$ ), and  $-5.7\text{\textperthousand}$ – $-1.4\text{\textperthousand}$  ( $450\text{ }^{\circ}\text{C}$ ) and to  $\delta\text{D} = -88\text{\textperthousand}$ – $-95\text{\textperthousand}$  ( $330$ – $450\text{ }^{\circ}\text{C}$ ) for the fluid isotopic compositions. The  $\delta^{18}\text{O}$  and  $\delta\text{D}$  compositions of the Chuncheon nephrite [54] signify that the nephrite-forming fluids are mainly meteoric water (Figure 6).

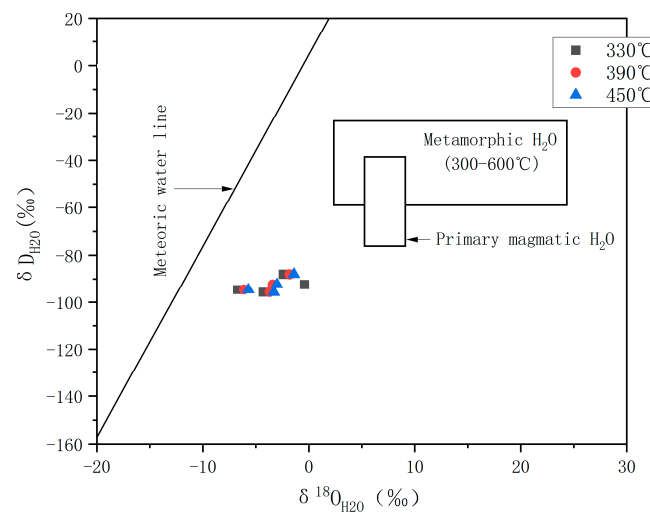


**Figure 6.**  $\delta\text{D}$  and  $\delta^{18}\text{O}_{\text{H}_2\text{O}}$  compositions of the hydrothermal fluids during the formation of the Chuncheon nephrite.

**Table 3.** Results of the hydrogen and oxygen isotope analyses of Chuncheon nephrite.

Samples	$\delta D_{V\text{-SMOW}} (\text{\textperthousand})$	$\delta^{18}\text{O}_{V\text{-SMOW}} (\text{\textperthousand})$	$\delta D_{\text{H}_2\text{O}}$ 330~450 °C	330 °C	$\delta^{18}\text{O}_{\text{H}_2\text{O}}$ 390 °C	450 °C
KC-1	-117	-4.8	-95	-4.3	-3.7	-3.3
KC-2	-114	-4.5	-92	-4.0	-3.4	-3.0
KC-3	-116	-7.2	-94	-6.7	-6.1	-5.7
KC-4	-109	-2.9	-88	-2.4	-1.8	-1.4

## 5. Discussion

The geochemical characteristics of the Chuncheon nephrite were further obtained by comparing its major elements, trace elements, REEs, and hydrogen and oxygen isotopes with those of dolomite-related nephrite of other geographic origins. The other geographic origin nephrites selected herein include Alamas in Xinjiang [39,41], Taksimo in Russia [2], Dahua in Guangxi [28–30], Panshi in Jilin [34], Tieli in Heilongjiang [45], Golmud in Qinghai [38], and Luodian in Guizhou [30–33].

### 5.1. Comparison of the Characteristics of the Main Elements

The Chuncheon nephrite samples were compared with the dolomite-related nephrite from different geographic origins in terms of the major elements (Table 4). The major element contents of the dolomite-related nephrite from different geographic origins are shown in Table 5.

The CaO content of the Chuncheon nephrite samples is low (11.16–13.05 wt%), and the MgO content in the Chuncheon nephrite is 22.52–25.03 wt%. The CaO and MgO contents of the Chuncheon nephrite and Alamas nephrite partially overlap (Figure 7a). While samples from Golmud, Qinghai; Panshi, Jilin; Dahua, Guangxi; and Tieli, Heilongjiang exhibit high CaO wt% with average CaO values of 13.59, 13.79, 13.80, and 13.88 wt%, respectively, which are generally higher than the theoretical tremolite CaO content (13.8 wt%). The Taksimo sample had the lowest CaO content (11.39–12.25 wt%).

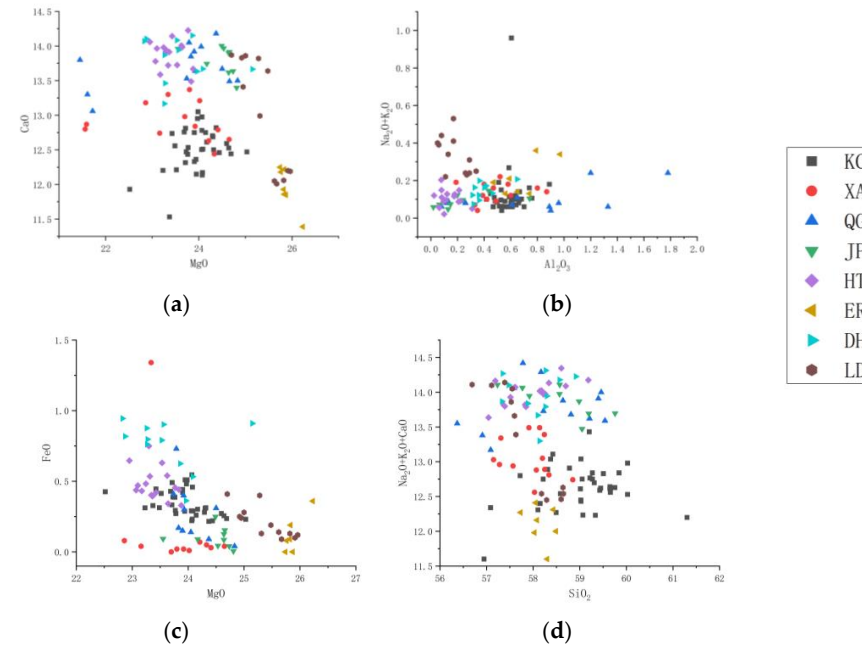


**Figure 7.** Comparison of the main elemental characteristics of dolomite-related nephrite from different geographic origins. (a) MgO wt% and CaO wt%; (b) Al<sub>2</sub>O<sub>3</sub> wt% and Na<sub>2</sub>O + K<sub>2</sub>O wt%; (c) MgO wt% and FeO wt%; (d) SiO<sub>2</sub> wt% and Na<sub>2</sub>O + K<sub>2</sub>O + CaO wt%. KC—Chuncheon, Korea; XA—Alamas, Xinjiang [41]; QG—Golmud, Qinghai [38]; JP—Panshi, Jilin [34]; HT—Tieli, Heilongjiang [45]; DH—Dahua, Guangxi [28].

**Table 4.** Average values of major element contents of dolomite-related nephrite from different geographic origins (wt%).

Samples	CaO	MgO	FeO	Al <sub>2</sub> O <sub>3</sub>	Na <sub>2</sub> O + K <sub>2</sub> O	SiO <sub>2</sub>	Na <sub>2</sub> O + K <sub>2</sub> O + CaO
KC	12.47	23.97	0.34	0.60	0.13	58.98	12.60
XA	12.92	23.85	0.15	0.43	0.13	58.06	13.05
QG	13.59	23.54	1.15	0.70	0.10	58.22	13.69
JP	13.79	24.47	0.10	0.23	0.09	58.56	13.88
HT	13.88	23.41	0.48	0.13	0.10	57.96	13.98
ER	11.95	25.87	0.13	0.68	0.21	58.16	12.17
DH	13.8	23.6	0.76	0.39	0.15	58.05	13.95
LD	12.99	25.39	0.21	0.19	0.33	57.82	13.33

Note: KC—Chuncheon, South Korea; XA—Alamas, Xinjiang [41]; QG—Golmud, Qinghai [38]; JP—Panshi, Jilin [34]; HT—Tieli, Heilongjiang [45]; ER—Taksimo, Russia [2]; DH—Dahua, Guangxi [28]; LD—Luodian, Guizhou [33].

**Table 5.** Main chemical composition data of the dolomite-related nephrite from different geographic origins (wt%).

Sample	SiO <sub>2</sub>	Al <sub>2</sub> O <sub>3</sub>	FeO	MgO	CaO	Na <sub>2</sub> O	K <sub>2</sub> O	MgO + FeO	Na <sub>2</sub> O + K <sub>2</sub> O	Na <sub>2</sub> O + K <sub>2</sub> O + CaO
XA-1	58.24	0.40	0.01	24.02	13.21	0.04	0.14	24.03	0.18	13.39
XA-2	58.14	0.39	0.02	23.80	13.37	0.05	0.07	23.82	0.12	13.49
XA-3	58.20	0.33	0.00	23.70	12.98	0.03	0.04	23.70	0.07	13.05
XA-4	58.07	0.35	0.02	23.92	12.84	0.00	0.04	23.94	0.04	12.88
XA-5	58.25	0.42	0.03	24.41	12.79	0.05	0.05	24.44	0.10	12.89
XA-6	58.34	0.58	0.07	24.21	12.63	0.08	0.10	24.28	0.18	12.81
XA-7	58.85	0.49	0.04	24.65	12.65	0.03	0.06	24.69	0.09	12.74
XA-8	58.03	0.60	0.05	24.33	12.44	0.04	0.08	24.38	0.12	12.56
XA-9	57.31	0.47	0.08	22.86	13.18	0.06	0.10	22.94	0.16	13.34
XA-10	57.28	0.52	0.04	23.16	12.74	0.00	0.22	23.20	0.22	12.96
XA-11	57.91	0.19	1.34	23.34	13.30	0.12	0.07	24.68	0.19	13.49
QG-1	57.59	0.61	0.30	23.93	13.99	0.06	0.01	24.23	0.07	14.06
QG-2	57.78	1.20	0.14	24.05	14.18	0.17	0.07	24.19	0.24	14.42
QG-3	59.54	0.13	0.09	24.37	13.50	0.06	0.03	24.46	0.09	13.59
QG-4	59.46	0.12	0.04	24.83	13.92	0.06	0.02	24.87	0.08	14.00
QG-5	59.40	0.08	0.15	23.90	13.85	0.04	0.02	24.05	0.06	13.91
QG-6	59.21	0.13	0.17	23.83	13.53	0.06	0.03	24.00	0.09	13.62
QG-7	58.22	0.89	0.41	23.74	13.67	0.02	0.04	24.15	0.06	13.73
QG-8	58.81	0.90	0.31	24.50	13.64	0.03	0.01	24.81	0.04	13.68
QG-9	58.17	1.78	0.40	23.92	14.05	0.17	0.07	24.32	0.24	14.29
QG-10	58.64	0.26	0.73	23.79	13.80	0.05	0.03	24.52	0.08	13.88
QG-11	56.91	0.96	5.45	21.45	13.30	0.04	0.04	26.90	0.08	13.38
QG-12	57.09	0.65	4.48	21.61	13.06	0.07	0.04	26.09	0.11	13.17
QG-13	56.37	1.33	3.22	21.72	13.49	0.03	0.03	24.94	0.06	13.55
JP-1	58.57	0.02	0.15	24.66	13.92	0.04	0.02	24.81	0.06	13.97
JP-2	57.77	0.24	0.04	24.53	13.97	0.05	0.04	24.58	0.10	14.07
JP-3	58.99	0.20	0.09	24.17	13.75	0.09	0.03	24.26	0.12	13.87
JP-4	57.92	0.13	0.09	24.64	13.90	0.02	0.02	24.72	0.05	13.95
JP-5	58.57	0.43	0.09	23.55	13.96	0.13	0.02	23.65	0.15	14.11
JP-6	59.19	0.15	0.13	24.64	13.62	0.06	0.02	24.77	0.07	13.69
JP-7	59.76	0.06	0.04	24.73	13.64	0.02	0.04	24.78	0.06	13.70
JP-8	59.05	0.06	0.01	24.81	13.40	0.04	0.04	24.82	0.07	13.47
JP-9	57.23	0.74	0.25	24.49	14.00	0.07	0.04	24.74	0.10	14.11
HT-1	58.60	0.02	0.46	23.77	14.23	0.09	0.03	24.22	0.12	14.35
HT-2	57.85	0.08	0.43	23.17	13.59	0.14	0.07	23.60	0.20	13.79
HT-3	58.70	0.08	0.48	23.25	13.98	0.07	0.04	23.73	0.11	14.09
HT-4	57.19	0.10	0.42	23.43	14.14	0.01	0.01	23.85	0.02	14.16
HT-5	57.39	0.12	0.33	23.88	13.67	0.06	0.06	24.21	0.13	13.80
HT-6	57.37	0.22	0.40	23.34	13.72	0.07	0.02	23.74	0.09	13.81
HT-7	58.14	0.10	0.54	23.32	13.93	0.07	0.02	23.85	0.09	14.02

**Table 5.** Cont.

Sample	SiO <sub>2</sub>	Al <sub>2</sub> O <sub>3</sub>	FeO	MgO	CaO	Na <sub>2</sub> O	K <sub>2</sub> O	MgO + FeO	Na <sub>2</sub> O + K <sub>2</sub> O	Na <sub>2</sub> O + K <sub>2</sub> O + CaO
HT-8	57.83	0.11	0.63	23.53	13.73	0.04	0.05	24.17	0.10	13.82
HT-9	59.18	0.18	0.65	22.95	14.06	0.09	0.03	23.60	0.12	14.18
HT-10	58.18	0.06	0.47	23.10	13.97	0.04	0.02	23.57	0.06	14.02
HT-11	57.51	0.08	0.44	23.07	13.78	0.10	0.05	23.51	0.15	13.93
HT-12	58.22	0.06	0.40	23.36	13.92	0.04	0.02	23.76	0.06	13.97
HT-13	58.34	0.18	0.54	23.63	14.01	0.07	0.06	24.17	0.13	14.13
HT-14	57.04	0.21	0.44	23.84	13.49	0.07	0.08	24.28	0.15	13.64
HT-15	57.62	0.21	0.34	23.64	13.99	0.06	0.02	23.99	0.09	14.07
HT-16	58.26	0.31	0.75	23.30	13.92	0.04	0.01	24.05	0.05	13.97
ER-1	58.30	0.59	0.36	26.23	11.39	0.21	0.00	26.59	0.21	11.60
ER-2	58.03	0.56	0.00	25.87	11.85	0.13	0.00	25.87	0.13	11.98
ER-3	58.49	0.65	0.19	25.83	11.86	0.06	0.08	26.02	0.14	12.00
ER-4	58.43	0.74	0.08	25.76	12.18	0.03	0.10	25.84	0.13	12.31
ER-5	58.08	0.79	0.00	25.74	12.25	0.23	0.13	25.74	0.36	12.61
ER-6	57.73	0.97	0.09	25.82	11.93	0.24	0.10	25.91	0.34	12.27
ER-7	58.05	0.47	0.19	25.83	12.22	0.19	0.00	26.02	0.19	12.41
DH-1	58.30	0.32	0.76	23.26	13.87	0.05	0.02	24.03	0.07	13.94
DH-2	58.57	0.36	0.79	23.53	14.08	0.05	0.04	24.32	0.10	14.18
DH-3	58.10	0.65	0.80	23.28	13.46	0.08	0.13	24.07	0.21	13.67
DH-4	58.14	0.46	0.88	23.26	13.17	0.05	0.08	24.14	0.13	13.30
DH-5	57.35	0.36	0.95	22.83	14.07	0.13	0.07	23.77	0.20	14.27
DH-6	58.92	0.36	0.82	22.87	14.11	0.05	0.07	23.69	0.12	14.23
DH-7	58.26	0.31	0.53	24.08	13.67	0.05	0.07	24.62	0.12	13.79
DH-8	57.47	0.33	0.90	23.56	13.94	0.12	0.04	24.46	0.16	14.10
DH-9	57.89	0.41	0.91	25.15	13.67	0.11	0.06	26.06	0.17	13.84
DH-10	58.27	0.40	0.63	23.86	14.15	0.12	0.05	24.48	0.16	14.31
DH-11	57.33	0.28	0.36	23.96	13.63	0.16	0.08	24.32	0.23	13.87
LD-1	57.55	0.27	0.40	25.28	13.82	0.23	0.00	25.68	0.23	14.05
LD-2	57.39	0.29	0.25	24.92	13.83	0.28	0.03	25.17	0.31	14.14
LD-3	57.11	0.29	0.28	25.00	13.86	0.24	0.00	25.28	0.24	14.10
LD-4	57.53	0.11	0.19	25.48	13.64	0.21	0.01	25.67	0.22	13.86
LD-5	56.69	0.26	0.41	24.70	13.87	0.24	0.00	25.11	0.24	14.11
LD-6	57.60	0.34	0.24	24.95	13.41	0.20	0.05	25.19	0.25	13.66
LD-7	58.60	0.17	0.14	25.62	12.05	0.41	0.00	25.76	0.41	12.46
LD-8	58.65	0.13	0.10	25.91	12.20	0.34	0.00	26.01	0.34	12.54
LD-9	57.63	0.05	0.13	25.31	12.99	0.29	0.11	25.44	0.40	13.39
LD-10	58.64	0.08	0.12	25.96	12.19	0.34	0.10	26.08	0.44	12.63
LD-11	58.29	0.06	0.13	25.82	12.06	0.33	0.06	25.95	0.39	12.45
LD-12	58.18	0.17	0.09	25.67	12.01	0.39	0.14	25.76	0.53	12.54

Note: XA—Alamas, Xinjiang [41]; QG—Golmud, Qinghai [38]; JP—Panshi, Jilin [34]; HT—Tieli, Heilongjiang [45]; ER—Taksimo, Russia [2]; DH—Dahua, Guangxi [28]; LD—Luodian, Guizhou [33].

Small amounts of Al can replace Mg and Fe, and small amounts of Na, K, and Mn can replace Ca, Mg, and Fe in the mineral. Moreover, the Al<sub>2</sub>O<sub>3</sub> wt% is negatively related to Na<sub>2</sub>O + K<sub>2</sub>O wt%. The increase in the Al and Na–K content indicates a high degree of hornblende metamorphism. The low Al<sub>2</sub>O<sub>3</sub> wt% (0.42–0.89 wt%) and Na<sub>2</sub>O + K<sub>2</sub>O wt% (0.04–0.96 wt%) contents of the Chuncheon nephrite samples indicate a low degree of metamorphism. The average content of Na<sub>2</sub>O + K<sub>2</sub>O wt% of the Luodian nephrite (0.33 wt%) is higher than that of the other geographic origins, indicating a high degree of metamorphism. The average Al<sub>2</sub>O<sub>3</sub> wt% content of the nephrite from Golmud, Qinghai (0.70 wt%) is higher than that of other geographic origins. The Al<sub>2</sub>O<sub>3</sub> content of all the deposits is less than 0.8 wt%. The Na<sub>2</sub>O + K<sub>2</sub>O content in all the deposits except Luodian nephrite is less than 0.3 wt%, indicating a low degree of metamorphism (Figure 7b).

In tremolite minerals, Mg<sup>2+</sup> and Fe<sup>2+</sup> can be substituted via complete isomorphism, and the MgO and FeO contents of different barite-type chondrites are negatively correlated (Figure 7c). The FeO content of the nephrite from different geographic origins is concen-

trated in the range of 0–1.34 wt%, and the MgO content is in the range of 21.45–26.23 wt%. The FeO (0.22–0.55 wt%) and MgO (22.52–25.03 wt%) contents of the Chuncheon nephrite are similar to those of nephrite from different geographic origins (Figure 7c). Both the Chuncheon nephrite and dolomite-related nephrite with different geographic origins exhibit high contents of Mg and low contents of Fe. The Taksimo nephrite has the highest MgO content (25.74–26.23 wt%), while the average FeO content of 0.13 wt% is lower than that of the other geographic origins.

The  $\text{Na}_2\text{O} + \text{K}_2\text{O} + \text{CaO}$  contents of nephrite from different geographic origins are concentrated in the range of 11.60–14.42 wt% (Figure 7d). Chuncheon nephrite has lower  $\text{Na}_2\text{O} + \text{K}_2\text{O} + \text{CaO}\%$  (11.34–13.43 wt%) and higher  $\text{SiO}_2\%$  (56.95–61.30 wt%) than nephrite from other geographic origins. The Chuncheon nephrite can be somewhat distinguished from nephrite samples from other geographic origins using  $\text{Na}_2\text{O} + \text{K}_2\text{O} + \text{CaO}\%$  and  $\text{SiO}_2\%$  (Figure 7d). The Taksimo nephrite has the lowest  $\text{Na}_2\text{O} + \text{K}_2\text{O} + \text{CaO}\%$  (11.60–12.61 wt%).

### 5.2. Comparison of Trace Element Characteristics

The Chuncheon nephrite samples were compared with dolomite-related nephrites from different geographic origins in terms of the trace element content (Table 6). The average values of the trace element content of dolomite-related nephrites from different geographic origins are presented in Table 7.

The trace element content of dolomite-related nephrite from different geographic origins is low and exhibits similarity. The Cr content of the Chuncheon nephrite is lower than that of nephrite from different geographic origins. The Daha nephrite generally has more trace elements, with Ni, Sr, Zr, Nb, Ba, Nd, Ta, and Th being higher than nephrite from other geographic origins.

The Alamas nephrite has the highest Rb and Cr contents among the nephrites of different geographic origins. Cr–Ni–Co content can be used to divide the genetic types of nephrites and is often used to distinguish between dolomite-related and serpentine-related nephrite [12,28,55,56]. Dolomite-related nephrite generally has low Cr, Ni, and Co contents, while the serpentine-related nephrite has high Cr, Ni, and Co contents. The Chuncheon nephrite has low Cr (0.48–1.99 ppm), Ni (9.13–16.69 ppm), and Co (0.065–0.462 ppm) contents. Since the Co content was not measured in the nephrite from some geographic origins, the Cr and Ni contents were used for the graphs. Comparison shows that the Cr and Ni contents of the Chuncheon nephrite are lower than those of dolomite-related nephrites from other geographic origins (Figure 8). The Cr, Ni, and Co contents of the dolomite-related nephrite from different geographic origins are 0–50, 0–40, and 0.80–83.65 ppm.

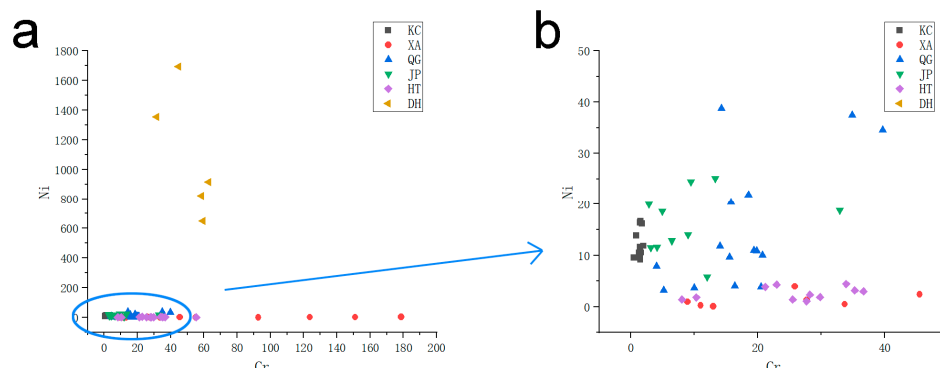


**Figure 8.** (a) Comparison of the Cr and Ni content of dolomite-related nephrite from different geographic origins. (b) Zoomed-in version of Figure 8a. KC—Chuncheon, Korea; XA—Alamas, Xinjiang [41]; QG—Golmud, Qinghai [38]; JP—Panshi, Jilin [34]; HT—Tieli, Heilongjiang [45]; DH—Daha, Guangxi [28].



**Table 7.** Comparison of the average values of the trace element characteristics of dolomite-related nephrites from different geographic origins.

Samples	Rb/Sr	U/Th	Sr/Ba
KC	0.11	4.03	29.13
XA	2.66	6.95	5.50
QG	0.13	7.92	1.72
JP	0.02	8.69	53.50
HT	0.01	6.30	37.42
DH	0.01	0.25	2.48

Note: KC—Chuncheon, South Korea; XA—Alamas, Xinjiang [41]; QG—Golmud, Qinghai [38]; JP—Panshi, Jilin [34]; HT—Tieli, Heilongjiang [45]; DH—Dahua, Guangxi [28].

U/Th can be used as an indicator of redox to judge the paleosedimentary environment; U/Th > 1.25 indicates an anaerobic environment; U/Th between 0.75 and 1.25 indicates a poor oxygen environment; and U/Th < 0.75 denotes an oxygen-rich environment [9]. Most of the nephrite from other geographic origins has a U/Th > 1.25, indicating that it formed in an anaerobic environment, and the U/Th of the Chuncheon nephrite is all >1.25 (1.68–10.06), which also signifies formation in an anaerobic environment. Only the U/Th of the Guangxi Dahua nephrite is generally lower than 0.75 (0.12–0.77), denoting formation in an aerobic environment.

Both Ba and Sr are chemically similar alkaline earth metals that behave differently in different environments. They can be used to assess the pH during mineralization, with Sr/Ba < 1 indicating an acidic mineralizing environment and Sr/Ba > 1 indicating an alkaline mineralizing environment [37]. Sr/Ba (9.81–48.66) > 1 for the Chuncheon nephrite indicates that it formed in an alkaline mineralizing environment. All the nephrites from other geographic origins have Sr/Ba (1.72–53.50) > 1, which also indicates that they formed in an alkaline environment.

The elemental variations in the Rb/Sr ratio indicate the degree of variable segregation crystallization in granitic magmas. The Rb/Sr ratio can be used to characterize the degree of segregation crystallization, alteration, and mineralization; the Rb/Sr values are high when mineralization occurs [57]. The average value of Rb/Sr of the Chuncheon nephrite is 0.11 (0.05–0.16), which is lower than that of Alamas (2.66) and Golmud (0.13).

### 5.3. Comparison of REE Characteristics

The Chuncheon nephrite samples were compared with the dolomite-related nephrites from other geographic origins in terms of the REE content (Table 8). The average values of the REE contents of dolomite-related nephrites from different geographic origins are presented in Table 9.

#### 5.3.1. Comparison of ΣREE Characteristics

The REE content of hydrothermal fluids in the genesis of nephrite deposits, whether magmatic hydrothermal fluids, metamorphic hydrothermal fluids, or groundwater hydrothermal fluids, is generally low. Therefore, the REE content of nephrite is mainly influenced by the surrounding rocks [37]. The nephrite from different geographic origins is surrounded by marble, and its REE characteristics are similar, with ΣREE content ranging from 2.13 to 44.01 ppm. The ΣREE content of the Chuncheon nephrite is 1.51–2.73 ppm, which is lower than the ΣREE content of nephrite from other geographic origins. Furthermore, the Luodian nephrite has the highest ΣREE content (25.89–91.81 ppm). LREE enrichment is generally observed in all the compared nephrite samples, with LREE/HREE concentrated in the range of 0.22–7.48. LREE enrichment is more intense in the Chuncheon nephrite, with LREE/HREE ranging from 4.13 to 9.04 (Figure 9).

**Table 8.** REEs of dolomite-related nephrites from different geographic origins (ppm).

Sample	La	Ce	Pr	Nd	Sm	Eu	Gd	Tb	Dy	Ho	Er	Tm	Yb	Lu	$\Sigma$ REE	LREE	HREE	LREE/HREE
XA-1	0.59	1.47	0.19	0.92	0.29	0.02	0.33	0.06	0.47	0.11	0.34	0.05	0.35	0.06	5.25	3.48	1.77	1.97
XA-2	0.58	1.09	0.17	0.77	0.21	0.02	0.25	0.05	0.36	0.08	0.23	0.04	0.23	0.04	4.12	2.84	1.28	2.22
XA-3	2.85	6.00	0.75	2.82	0.60	0.07	0.51	0.08	0.56	0.12	0.34	0.05	0.35	0.05	15.15	13.09	2.06	6.35
XA-4	0.38	0.55	0.06	0.25	0.10	0.01	0.18	0.05	0.46	0.13	0.42	0.07	0.42	0.06	3.14	1.35	1.79	0.75
XA-5	0.90	2.50	0.38	1.85	0.62	0.03	0.74	0.16	1.26	0.31	0.96	0.16	1.10	0.17	11.14	6.28	4.86	1.29
XA-6	1.47	2.68	0.37	1.41	0.37	0.01	0.38	0.07	0.51	0.12	0.34	0.05	0.31	0.05	8.14	6.31	1.83	3.45
XA-7	0.20	0.39	0.06	0.34	0.17	0.01	0.30	0.07	0.54	0.12	0.32	0.04	0.26	0.04	2.86	1.17	1.69	0.69
XA-8	26.40	38.72	3.44	10.45	1.36	0.28	1.35	0.17	1.01	0.21	0.63	0.09	0.61	0.10	84.82	80.65	4.17	19.34
XA-9	0.45	0.94	0.12	0.55	0.18	0.02	0.28	0.06	0.53	0.13	0.38	0.05	0.29	0.04	4.02	2.26	1.76	1.28
XA-10	0.25	0.67	0.12	0.71	0.32	0.04	0.46	0.09	0.69	0.16	0.47	0.07	0.37	0.05	4.47	2.11	2.36	0.89
XA-11	0.17	0.44	0.08	0.44	0.22	0.03	0.35	0.08	0.57	0.13	0.37	0.05	0.31	0.04	3.28	1.38	1.90	0.73
XA-12	13.57	19.90	1.64	4.36	0.66	0.02	0.73	0.11	0.75	0.18	0.54	0.09	0.72	0.10	43.37	40.15	3.22	12.47
XA-AVG	3.98	6.28	0.62	2.07	0.43	0.05	0.49	0.09	0.64	0.15	0.45	0.07	0.44	0.07	15.81	13.42	2.39	4.29
QG-1	3.37	6.61	0.56	2.16	0.52	0.13	0.55	0.12	0.75	0.14	0.38	0.07	0.44	0.06	15.86	13.42	2.51	5.35
QG-2	2.54	5.62	0.54	1.48	0.43	0.11	0.46	0.10	0.66	0.13	0.31	0.06	0.39	0.05	12.88	10.09	2.17	4.65
QG-3	0.45	1.48	0.14	0.59	0.12	0.02	0.12	0.02	0.11	0.02	0.06	0.01	0.06	0.01	3.21	2.50	0.40	6.25
QG-4	0.72	1.74	0.14	0.57	0.13	0.02	0.11	0.02	0.12	0.02	0.06	0.01	0.08	0.01	3.75	3.12	0.45	6.93
QG-5	0.57	1.44	0.11	0.48	0.11	0.03	0.10	0.02	0.11	0.02	0.06	0.01	0.07	0.01	3.14	2.54	0.40	6.35
QG-6	0.16	0.75	0.05	0.18	0.05	0.01	0.08	0.02	0.16	0.04	0.21	0.05	0.48	0.09	2.33	0.81	1.13	0.72
QG-7	0.11	0.63	0.02	0.09	0.03	0.01	0.04	0.01	0.07	0.02	0.07	0.02	0.12	0.02	1.26	0.39	0.36	1.08
QG-8	0.05	0.43	0.02	0.10	0.02	0.01	0.06	0.02	0.12	0.03	0.10	0.03	0.20	0.03	1.22	0.29	0.58	0.50
QG-9	0.14	0.36	0.02	0.10	0.02	0.01	0.02	0.00	0.02	0.00	0.02	0.00	0.01	0.00	0.72	0.53	0.09	5.89
QG-10	0.13	0.37	0.02	0.10	0.03	0.01	0.03	0.00	0.03	0.01	0.02	0.00	0.02	0.00	0.77	0.53	0.11	4.82
QG-11	0.17	0.43	0.05	0.17	0.04	0.01	0.03	0.01	0.03	0.01	0.01	0.00	0.02	0.00	0.98	0.82	0.11	7.45
QG-12	0.11	0.19	0.03	0.13	0.03	0.00	0.02	0.00	0.03	0.01	0.02	0.00	0.01	0.00	0.58	0.49	0.09	5.44
QG-13	0.15	0.29	0.04	0.17	0.04	0.01	0.04	0.01	0.04	0.01	0.02	0.00	0.03	0.00	0.85	0.69	0.15	4.60
QG-14	0.06	0.08	0.01	0.06	0.02	0.00	0.02	0.00	0.02	0.00	0.01	0.00	0.01	0.00	0.29	0.23	0.07	3.29
QG-15	0.08	0.11	0.01	0.05	0.02	0.00	0.02	0.00	0.02	0.01	0.01	0.00	0.02	0.00	0.35	0.27	0.09	3.00
QG-AVG	0.59	1.37	0.12	0.43	0.11	0.03	0.11	0.02	0.15	0.03	0.09	0.02	0.13	0.02	3.21	2.45	0.58	4.42
JP-1	0.31	0.33	0.13	0.90	0.43	0.12	0.36	0.14	0.63	0.16	0.25	0.04	0.07	0.03	3.90	2.23	1.67	1.33
JP-2	0.84	0.70	0.19	1.03	0.54	0.04	0.31	0.08	0.45	0.13	0.24	0.04	0.19	0.03	4.82	3.34	1.48	2.26
JP-3	0.64	0.58	0.19	1.10	0.30	0.03	0.28	0.13	0.71	0.20	0.50	0.06	0.36	0.05	5.12	2.83	2.29	1.24
JP-4	0.30	0.17	0.06	0.41	0.18	0.01	0.06	0.05	0.15	0.02	0.22	0.00	0.15	0.04	1.83	1.13	0.70	1.62
JP-5	0.33	0.28	0.12	0.88	0.39	0.10	0.14	0.06	0.09	0.05	0.22	0.05	0.22	0.03	2.95	2.09	0.86	2.44
JP-6	1.20	0.61	0.17	0.47	0.14	0.06	0.18	0.03	0.27	0.05	0.13	0.03	0.33	0.03	3.70	2.65	1.05	2.53

**Table 8.** Cont.

Sample	La	Ce	Pr	Nd	Sm	Eu	Gd	Tb	Dy	Ho	Er	Tm	Yb	Lu	$\Sigma$ REE	LREE	HREE	LREE/HREE
JP-7	0.34	0.40	0.15	0.87	0.05	0.07	0.05	0.07	0.21	0.04	0.24	0.06	0.09	0.04	2.68	1.87	0.80	2.33
JP-8	0.37	0.60	0.14	0.50	0.33	0.08	0.19	0.04	0.23	0.08	0.13	0.04	0.08	0.03	2.85	2.02	0.83	2.44
JP-9	0.40	0.64	0.19	0.82	0.23	0.01	0.25	0.05	0.45	0.11	0.34	0.05	0.28	0.01	3.81	2.29	1.53	1.50
JP-10	0.49	0.63	0.15	0.65	0.16	0.13	0.21	0.05	0.37	0.08	0.21	0.05	0.43	0.04	3.66	2.21	1.45	1.52
JP-AVG	0.52	0.49	0.15	0.76	0.28	0.06	0.20	0.07	0.36	0.09	0.25	0.04	0.22	0.03	3.53	2.27	1.27	1.92
HT-1	0.52	1.52	0.17	0.88	0.13	0.05	0.07	0.01	0.17	0.02	0.09	0.01	0.04	0.01	3.70	3.26	0.44	7.48
HT-2	0.32	1.22	0.12	0.59	0.13	0.04	0.19	0.03	0.13	0.03	0.06	0.01	0.08	0.01	2.95	2.42	0.53	4.56
HT-3	0.34	1.53	0.22	0.83	0.20	0.08	0.21	0.03	0.18	0.03	0.10	0.01	0.07	0.00	3.85	3.21	0.64	5.00
HT-4	0.58	1.57	0.23	0.79	0.26	0.04	0.22	0.04	0.19	0.03	0.10	0.02	0.09	0.02	4.18	3.47	0.71	4.86
HT-5	0.44	1.56	0.15	0.80	0.22	0.04	0.00	0.04	0.06	0.02	0.14	0.02	0.14	0.01	3.66	3.22	0.44	7.30
HT-6	0.27	1.06	0.10	0.90	0.16	0.07	0.14	0.06	0.27	0.05	0.09	0.02	0.06	0.02	3.27	2.56	0.72	3.57
HT-7	0.47	2.29	0.26	0.51	0.17	0.09	0.32	0.02	0.23	0.06	0.19	0.03	0.12	0.01	4.77	3.79	0.99	3.84
HT-8	0.45	1.34	0.13	0.58	0.19	0.07	0.14	0.03	0.16	0.05	0.13	0.00	0.07	0.01	3.34	2.75	0.59	4.67
HT-9	0.67	1.84	0.25	0.81	0.16	0.05	0.18	0.02	0.17	0.03	0.11	0.01	0.07	0.01	4.38	3.78	0.60	6.34
HT-10	0.30	1.14	0.17	0.66	0.14	0.04	0.07	0.02	0.15	0.02	0.08	0.01	0.06	0.01	2.86	2.44	0.42	5.84
HT-11	0.80	2.28	0.36	1.57	0.42	0.05	0.50	0.06	0.36	0.06	0.21	0.02	0.09	0.02	6.81	5.47	1.34	4.09
HT-12	1.17	3.65	0.51	2.15	0.62	0.12	0.59	0.10	0.74	0.15	0.51	0.05	0.43	0.04	10.84	8.23	2.61	3.15
HT-AVG	0.53	1.75	0.22	0.92	0.23	0.06	0.22	0.04	0.23	0.05	0.15	0.02	0.11	0.02	4.55	3.72	0.84	5.06
DH-1	0.62	1.20	0.16	0.57	0.04	0.01	0.16	0.02	0.13	0.03	0.05	0.01	0.03	0.00	4.05	2.60	0.43	0.18
DH-2	3.52	1.18	0.53	2.49	0.43	0.13	0.51	0.07	0.43	0.11	0.25	0.02	0.15	0.03	3.99	8.28	1.57	0.22
DH-3	3.70	1.19	0.54	2.27	0.57	0.11	0.34	0.08	0.53	0.08	0.30	0.03	0.27	0.04	3.04	8.38	1.67	6.11
DH-4	0.48	0.86	0.12	0.47	0.11	0.09	0.17	0.04	0.35	0.12	0.33	0.05	0.33	0.05	9.87	2.13	1.44	5.24
DH-5	0.86	0.43	0.18	1.33	0.34	0.06	0.58	0.12	0.48	0.15	0.32	0.04	0.20	0.00	10.04	3.20	1.89	5.06
DH-6	0.38	0.21	0.08	0.39	0.20	0.01	0.24	0.06	0.41	0.13	0.46	0.05	0.23	0.03	3.57	1.27	1.61	1.49
DH-7	0.28	0.40	0.05	0.13	0.12	0.02	0.11	0.00	0.06	0.01	0.03	0.01	0.06	0.00	5.10	1.00	0.28	1.69
DH-AVG	1.41	0.78	0.24	1.09	0.26	0.06	0.30	0.06	0.34	0.09	0.25	0.03	0.18	0.02	5.67	3.84	1.27	2.86
LD-1	8.48	8.44	1.66	6.74	1.73	0.49	1.71	0.33	2.59	0.47	1.05	0.14	0.92	0.13	34.88	27.54	7.34	5.28
LD-2	7.32	3.84	1.40	5.71	1.14	0.25	1.46	0.21	1.53	0.36	1.24	0.17	1.11	0.15	25.89	19.66	6.23	4.48
LD-3	6.61	3.58	1.50	7.64	1.37	0.34	1.78	0.27	1.56	0.28	0.62	0.09	0.49	0.08	26.21	21.04	5.17	6.92
LD-4	6.31	6.81	1.74	6.21	1.24	1.19	1.24	0.22	1.38	0.27	0.84	0.15	0.93	0.14	41.28	23.50	5.16	4.55
LD-5	12.03	17.23	3.19	11.82	2.52	2.18	2.45	0.47	3.26	0.69	2.17	0.41	2.51	0.39	91.81	48.96	12.34	3.97
LD-AVG	8.15	7.98	1.90	7.62	1.60	0.89	1.73	0.30	2.06	0.41	1.18	0.19	1.19	0.18	44.01	28.14	7.25	5.04

Note: XA—Alamas, Xinjiang [41]; QG—Golmud, Qinghai [38]; JP—Panshi, Jilin [34]; HT—Tieli, Heilongjiang [45]; DH—Dahua, Guangxi [28]; LD—Luodian, Guizhou [30,33]; AVG—the average value of REEs.

**Table 9.** Average values of REEs in dolomite-related nephrites of different geographic origins.

Samples	$\Sigma$ REE	LREE	HREE	LREE/HREE	$\delta$ Eu	$\delta$ Ce	$(La/Sm)_N$	$(Sm/Ho)_N$	$(Gd/Lu)_N$
KC	2.13	1.83	0.30	6.23	1.06	1.46	10.17	1.66	1.06
XA	15.81	13.42	2.39	4.29	0.25	1.46	3.35	1.00	0.96
QG	3.21	2.45	0.58	4.42	0.74	2.19	2.78	1.26	0.90
JP	3.53	2.27	1.27	1.92	1.16	0.73	1.77	1.36	0.90
HT	4.55	3.72	0.84	5.06	0.99	2.38	1.54	2.01	2.56
DH	5.67	3.84	1.27	2.86	0.71	0.71	3.71	1.53	1.18
LD	44.01	28.14	7.25	5.04	1.53	0.66	3.27	1.48	1.54

Note: KC—Chuncheon, South Korea; XA—Alamas, Xinjiang [41]; QG—Golmud, Qinghai [38]; JP—Panshi, Jilin [34]; HT—Tieli, Heilongjiang [45]; DH—Dahua, Guangxi [28]; LD—Luodian, Guizhou [30,33].

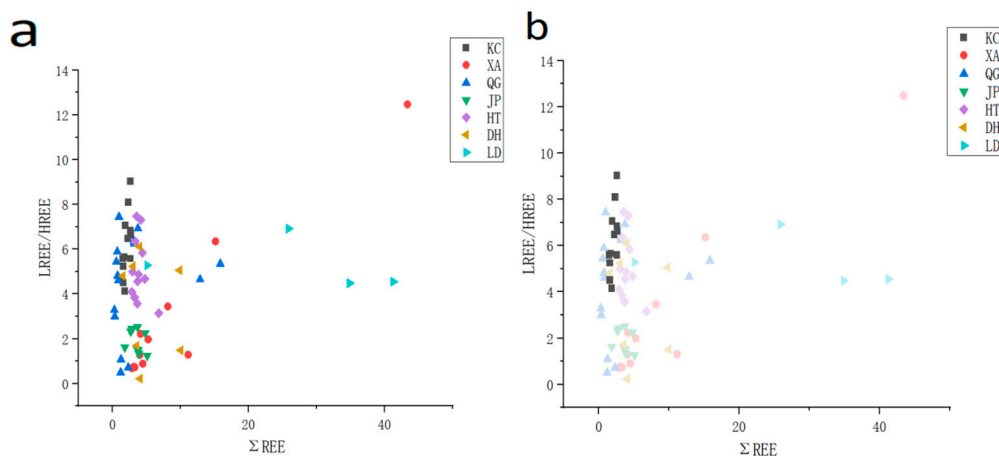


**Figure 9.** (a) Comparison of  $\Sigma$ REE and LREE/HREE for nephrite from different geographic origins. (b) The  $\Sigma$ REE and LREE/HREE content of Chuncheon nephrite. KC—Chuncheon, South Korea; XA—Alamas, Xinjiang [41]; QG—Golmud, Qinghai [38]; JP—Panshi, Jilin [34]; HT—Tieli, Heilongjiang [45]; DH—Dahua, Guangxi [28]; LD—Luodian, Guizhou [30,33].

### 5.3.2. $\delta$ Eu and $\delta$ Ce

The anomalies of elements Eu and Ce ( $\delta$ Eu and  $\delta$ Ce) can be analyzed for their genetic geographic origins and their geochemical backgrounds (Figure 10). The Chuncheon nephrite  $\delta$ Ce (1.31–1.63) has a weak positive anomaly, and  $\delta$ Eu (0.11–3.53) widely varies with both positive and negative anomalies. The  $\delta$ Eu and  $\delta$ Ce values of the Chuncheon nephrite are closest to those of the Alamas nephrite, but the Chuncheon nephrite has positive  $\delta$ Eu anomalies while the Alamas nephrite has no positive  $\delta$ Eu anomalies. The  $\delta$ Eu and  $\delta$ Ce values of the Golmud nephrite and Tieli nephrite are close to each other, exhibiting positive  $\delta$ Ce anomalies and weak positive and negative  $\delta$ Eu anomalies. The  $\delta$ Ce anomalies are negative in the Panshi, Dahua, and Luodian, while the  $\delta$ Eu anomalies are both positive and negative, and the degree of anomalies is strong.

### 5.3.3. $(La/Sm)_N$ , $(Sm/Ho)_N$ , $(Gd/Lu)_N$

The REE content of the nephrite samples from different geographic origins was normalized using the Boynton chondrite [50]. The  $(La/Sm)_N$ ,  $(Sm/Ho)_N$ , and  $(Gd/Lu)_N$  values were determined to explore the degree of differentiation among light, medium, and heavy REEs in the samples (Figure 11). All the samples exhibited a more pronounced differentiation of LREEs and a less pronounced differentiation of medium and heavy REEs. The Chuncheon nephrite exhibited a significantly higher degree of LREE differentiation, a greater difference in the degree of medium REE differentiation, and a low degree of HREE differentiation. Particularly, the average  $(La/Sm)_N$  value of the Chuncheon nephrite (10.17) is significantly higher than that of nephrite from other geographic origins (1.54–3.71).

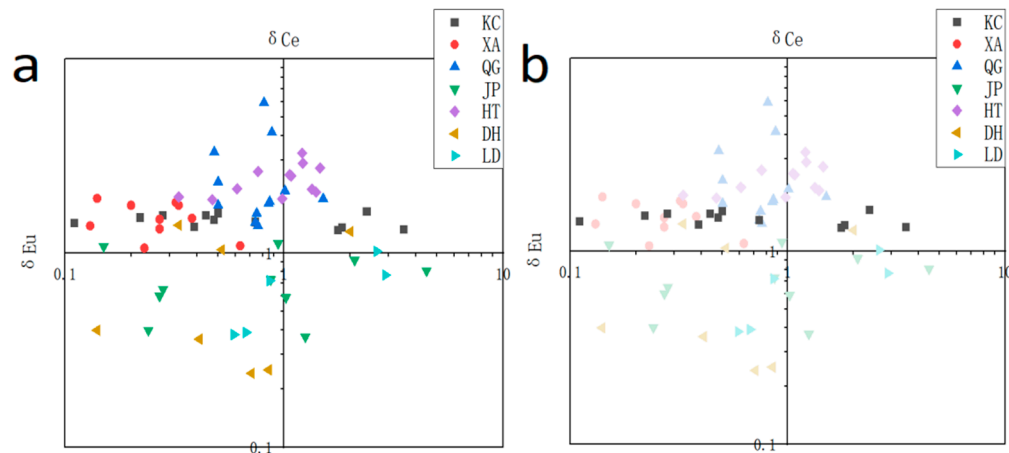


**Figure 10.** (a) Comparison of  $\delta\text{Eu}$  and  $\delta\text{Ce}$  values of nephrite from different geographic origins. (b) The  $\delta\text{Eu}$  and  $\delta\text{Ce}$  values of Chuncheon nephrite. KC—Chuncheon, South Korea; XA—Alamas, Xinjiang [41]; QG—Golmud, Qinghai [38]; JP—Panshi, Jilin [34]; HT—Tieli, Heilongjiang [45]; DH—Dahua, Guangxi [28]; LD—Luodian, Guizhou [30,33].

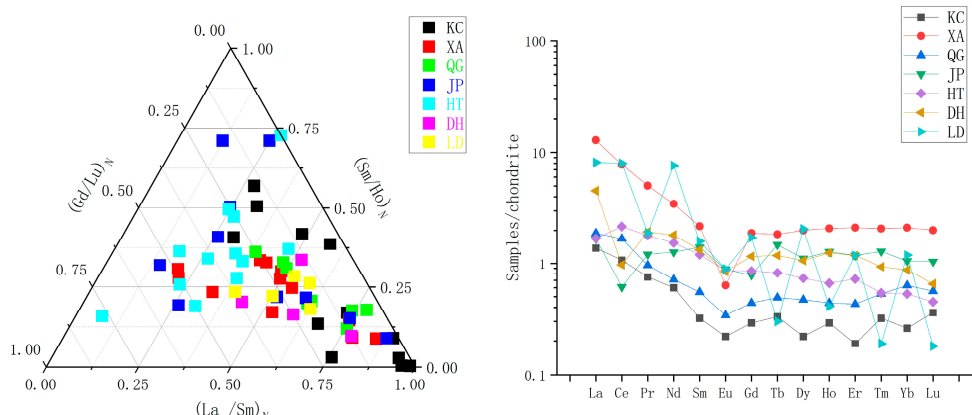


**Figure 11.** Comparison of REE characteristics of nephrite from different geographic origins. KC—Chuncheon, South Korea; XA—Alamas, Xinjiang [41]; QG—Golmud, Qinghai [38]; JP—Panshi, Jilin [34]; HT—Tieli, Heilongjiang [45]; DH—Dahua, Guangxi [28]; LD—Luodian, Guizhou [30,33].

The REE data in the nephrite samples from different geographic origins are standardized, and an REE/chondrite normalized distribution pattern is constructed (Figure 11). The distribution pattern of the REEs is skewed to the right for all the provenances, and the distribution pattern of REEs for the Chuncheon nephrite is also skewed to the right, indicating that LREEs are more enriched in the dolomite-related nephrite samples. The REE data from different deposits can be used to identify the geographic origins of dolomite-related nephrites (Figure 12).

$\text{Pr}_N$  (0.50–1.08),  $\text{Nd}_N$  (0.33–0.93),  $\text{Sm}_N$  (0.04–0.84),  $\text{Yb}_N$  (0.11–0.44), and  $\text{Dy}_N$  (0.004–0.047) of the REEs in the Chuncheon nephrite samples have low values and a small fluctuation range. Figure 13 displays the plots for  $\text{Pr}_N\text{--Sm}_N$ ,  $\text{Nd}_N\text{--Yb}_N$ ,  $\text{Nd}_N\text{--Sm}_N$ , and  $\text{Nd}_N\text{--Dy}_N$ . In the figure, the Chuncheon nephrite samples are clustered together and do not considerably overlap with the nephrite samples of other geographic origins, differentiating Chuncheon nephrites from other dolomite-related nephrites.

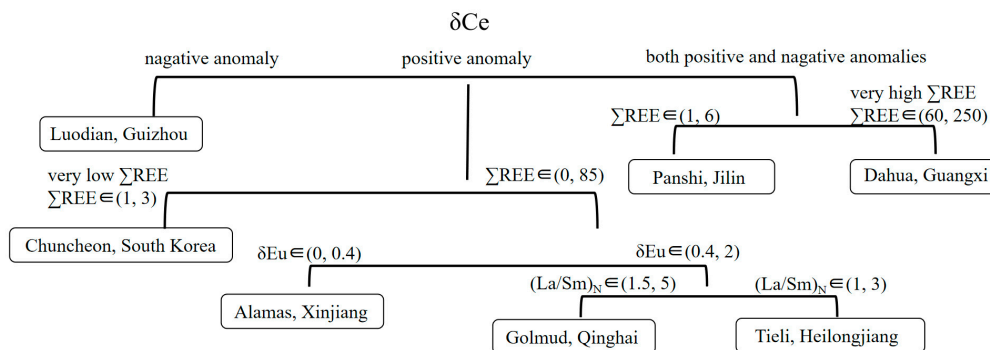


**Figure 12.** Identification of nephrite geographic origins using REEs.

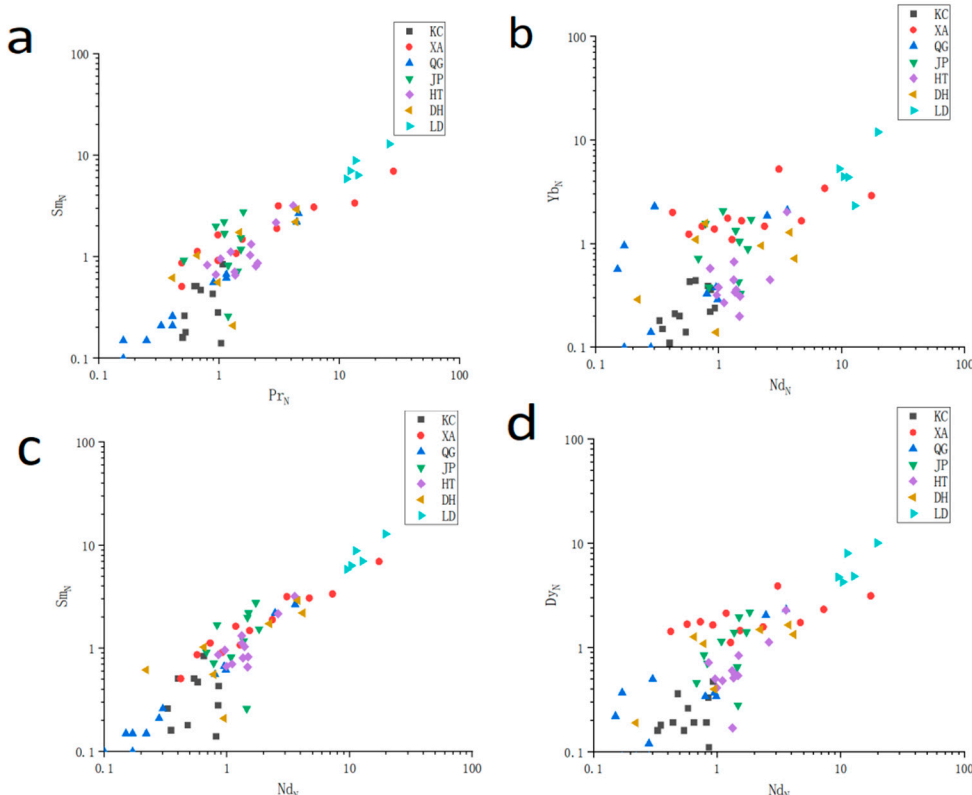


**Figure 13.** Comparison of the standardization of REEs of different geographic origins. (a)  $\text{Pr}_N\text{-Sm}_N$ ; (b)  $\text{Nd}_N\text{-Yb}_N$ ; (c)  $\text{Nd}_N\text{-Sm}_N$ ; (d)  $\text{Nd}_N\text{-Dy}_N$ . KC—Chuncheon, South Korea; XA—Alamas, Xinjiang [41]; QG—Golmud, Qinghai [38]; JP—Panshi, Jilin [34]; HT—Tieli, Heilongjiang [45]; DH—Dahua, Guangxi [28]; LD—Luodian, Guizhou [30,33].

#### 5.4. Hydrogen and Oxygen Isotope Characteristics of Nephrites from Different Geographic Origins

The hydrogen–oxygen isotopic compositions of nephrite samples from different geographic origins are shown in Table 10 [5,17,41]. Nephrite samples from Kunlun Mountains (China), Wyoming (USA), Cowell (Australia), Alamas (Xinjiang), and Złoty Stok (Poland) are all dolomite-related nephrite deposits.

The  $\delta D$  values of nephrite of different geographic origins ranged from  $-124\text{\textperthousand}$  to  $-56\text{\textperthousand}$  and the  $\delta^{18}\text{O}$  values ranged from  $-9.9\text{\textperthousand}$  to  $10.4\text{\textperthousand}$ ; both  $\delta D$  and  $\delta^{18}\text{O}$  values are low. The  $\delta D$  values of the Chuncheon nephrite are concentrated between  $-117\text{\textperthousand}$  and  $-105\text{\textperthousand}$ , and the  $\delta^{18}\text{O}$  values are concentrated between  $-9.9\text{\textperthousand}$  and  $-2.9\text{\textperthousand}$ . The  $\delta D$  and  $\delta^{18}\text{O}$  values are generally lower than those of dolomite-related nephrite from other geographic origins. Assuming a mineralization temperature of  $330\text{ }^{\circ}\text{C}$ , dolomite-related nephrite mineralizing fluids are mainly atmospheric water; Alamas mineralizing fluids are atmospheric water mixed with magmatic water; and Złoty Stok and Cowell, Australia

mineralizing fluids are metamorphic water (Figure 14). The  $\delta^{18}\text{O}$  content of Chuncheon nephrite is significantly lower than that of other dolomite-related nephrites, which is highly related to the geological genesis and formation mode of Chuncheon nephrite. Although it has generally been considered that dolomite-related nephrite forms at the contacts between granite/granodiorite and dolomitic marble, Chuncheon nephrite is located at the contact between calc-silicate rocks and amphibole schist and has no direct contact with dolomitic marble or granite. Therefore, it is a special kind of dolomite-related nephrite that was produced by the replacement of the calc-silicate rocks. The very low  $\delta^{18}\text{O}$  content of Chuncheon nephrite is also influenced by calc-silicate rocks. Carbonate within calc-silicate rocks and carbonate within marbles in direct contact with calc-silicate rocks are distinctly lower in oxygen isotope composition [17].

**Table 10.** Hydrogen and oxygen isotopes of dolomite-related nephrites from different geographic origins.

Sample	$\delta\text{D}$	$\delta^{18}\text{O}$	Sample	$\delta\text{D}$	$\delta^{18}\text{O}$	Sample	$\delta\text{D}$	$\delta^{18}\text{O}$
KC-1	-117	-4.8	NE-9	-109	-9.2	XA-2	-83	3.2
KC-2	-114	-4.5	CA-1	-57	3.4	XA-3	-93	6.1
KC-3	-116	-7.2	WU-1	-56	1.5	XA-4	-89	4.6
KC-4	-109	-2.9	TC-1	-108	2.3	XA-5	-85	3.5
NE-1	-108	-8.7	TC-2	-110	0.5	XA-6	-85	3.6
NE-2	-114	-8.4	TC-3	-124	0.6	XA-7	-94	6.2
NE-3	-105	-9.9	ZS-1	-76	10.2	XA-8	-90	4.1
NE-4	-107	-9.0	ZS-2	-76	8.3	XA-9	-85	3.6
NE-5	-108	-8.2	ZS-3	-77	10.4	XA-10	-91	4.9
NE-6	-112	-8.6	ZS-4	-74	10.2	XA-11	-90	4.8
NE-7	-109	-8.9	XA-1	-86	3.8	XA-12	-86	3.8
NE-8	-110	-9.3						

Note: KC—Chuncheon, Korea; NE—Chuncheon, Korea [17]; CA—Cowell, Australia; WU—Wyoming, USA; TC—Kunlun Mountains, China; ZS—Złoty Stok, Poland; XA—Alamas, Xinjiang.

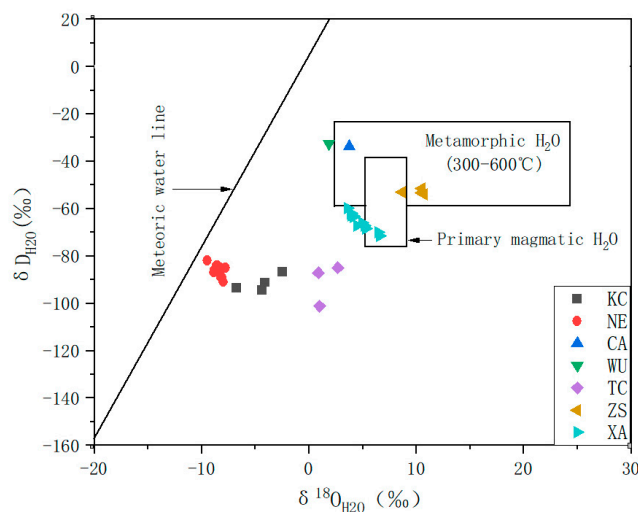


**Figure 14.** Hydrogen and oxygen isotope content characteristics of dolomite-related nephrite from different geographic origins. KC—Chuncheon, Korea; NE—Chuncheon, Korea [17]; CA—Cowell, Australia; WU—Wyoming, USA; TC—Kunlun Mountains, China; ZS—Złoty Stok, Poland; XA—Alamas, Xinjiang.

##### 5.5. Discussion of Mineral-Forming Material Sources

Yui and Kwon argued that the Chuncheon nephrite deposit is a product of fluid circulation at the contact between dolomitic barite and hornblende schist [17]. Feng et al. considered the dolomitic marble as the host rock (a Ca and Mg source) and speculated that the high Si content in the hot water solution ultimately stems from the black mica

schist connecting the upper part of the biotite schist zone [19]. Park and Noh found that the nephrite samples have Sr and Pb isotopic ratios similar to the Kyeonggi gneiss complex within which the deposit is located, suggesting the important role of crustal circulating water in the genesis of the deposit. The meteoric water supplied Sr and Pb by leaching the rocks surrounding the ore deposits [14].

Metamorphic rocks, as products of early-formed rocks subjected to late metamorphism, often exhibit petrographic characteristics depending on the composition of the original rock (igneous and sedimentary). Although the metamorphism process changes the mineral composition and structural configuration of the original rock, it only slightly changes the main chemical composition of the original rock. Therefore, the petrogeochemical characteristics of metamorphic rocks, to a certain extent, directly reflect certain chemical composition characteristics of the original rock. The Chuncheon nephrite deposit and surrounding rocks are characterized by zonation, from bottom to top as a dolomitic marble zone, a calc-silicate zone, a nephrite zone, a chlorite zone, an amphibole schist zone, a biotite schist zone, and a gneiss zone (Figure 2). The nephrite belt is in direct contact with the calc-silicate zone, chlorite zone, and amphibole schist zone. The biotite schist is rich in biotite minerals, thus exhibiting high Fe content and low Si content characteristics [58,59]. Gneisses are generally characterized by high Si content and low Fe content [42]. The chemical composition of the Chuncheon nephrite exhibits high Mg and Si content and low Fe and Ca content characteristics, which is close to that of gneisses, and the Sr and Pb isotope ratios of the Chuncheon nephrite are similar to those of the Kyeonggi gneiss, where the deposit is located [14]. Although the nephrite belt is not in direct contact with the gneiss belt, the chemical composition proves that gneiss formation is a necessary factor for nephrite formation. The genetic material source of the Chuncheon nephrite may be related to the amphibole schist, biotite schist, and gneissic miscellaneous rocks, but the contribution of the Chuncheon granite to the mineralization cannot be excluded. Further in-depth studies on the genesis of Chuncheon nephrite are required.

## 6. Conclusions

(1) The Chuncheon nephrite mainly comprises tremolite. The texture is mainly felt-like fibroblastic texture, pseudomorphic metasomatic texture, and secondary filling texture. The pseudomorphic metasomatic texture is a unique texture feature of the Chuncheon nephrite.

(2) The Chuncheon nephrite exhibits high Mg and Si content and low Fe and Ca content characteristics. The high  $Mg^{2+}/(Mg^{2+} + Fe^{2+})$  values, low Cr–Ni–Co content, and the rightward sloping distribution pattern of REEs indicate that the Chuncheon nephrite is dolomite-related nephrite. Its green color deepens with increasing  $Fe^{2+}$  content. The low  $Al_2O_3$  and  $Na_2O + K_2O$  contents indicate that the Chuncheon nephrite formed at low temperatures. The U/Th and Sr/Ba ratios indicate that the Chuncheon nephrite formed in an anaerobic alkaline environment. Moreover, the Rb/Sr ratio indicates its low mineralization. The hydrogen and oxygen isotope contents indicate that the Chuncheon nephrite mineralizing fluid was atmospheric water.

(3) Compared to other dolomite-related nephrites, Chuncheon nephrite has lower  $Na_2O + K_2O + CaO$  wt% (11.34–13.43 wt%) and higher  $SiO_2$  wt% (56.95–61.30 wt%). Consequently, it can be distinguished from nephrites from other geographic origins using  $Na_2O + K_2O + CaO$  wt% and  $SiO_2$  wt% map partitioning. The Cr content of Chuncheon nephrite is lower than that of other dolomite-related nephrites in terms of the trace elements. In terms of REEs, the Chuncheon nephrite LREEs are highly differentiated and higher than those of nephrites from other geographic origins, with lower and less fluctuating values of  $Pr_N$  (0.50–1.08),  $Nd_N$  (0.33–0.93),  $Sm_N$  (0.04–0.84),  $Yb_N$  (0.11–0.44), and  $Dy_N$  (0.004–0.047). The  $Pr_N$ – $Sm_N$ ,  $Nd_N$ – $Yb_N$ ,  $Nd_N$ – $Sm_N$ , and  $Nd_N$ – $Dy_N$  cast diagrams were used to distinguish Chuncheon nephrite from other dolomite-related nephrites. In terms of the hydrogen and oxygen isotopes, the  $\delta^{18}O$  and  $\delta D$  contents of Chuncheon nephrite are lower than those of dolomite-related nephrites from other geographic origins. The in  $\delta^{18}O$  and  $\delta D$  projec-

tion map partitioning was used to distinguish Chuncheon nephrite from dolomite-related nephrites from other geographic origins.

**Author Contributions:** Data curation, M.L.; writing—original draft preparation, N.L. and Q.P.; supervision, F.B. All authors have read and agreed to the published version of the manuscript.

**Funding:** This research received no external funding.

**Data Availability Statement:** No data was used for the research described in the article.

**Acknowledgments:** We thank the Institute of Geology and Geophysics of the Chinese Academy of Sciences for its help in sample testing.

**Conflicts of Interest:** The authors declare that they have no known competing financial interests or personal relationships that could have appeared to influence the work reported in this paper.

## References

- Burtseva, M.; Ripp, G.; Posokhov, V.; Murzintseva, A. Nephrites of East Siberia: Geochemical features and problems of genesis. *Russ. Geol. Geophys.* **2015**, *56*, 402–410. [[CrossRef](#)]
- Liu, X.F. Gemological and Mineralogical Study of White Nephrite from Dakeximu Region in Russia. Master’s Thesis, China University of Geosciences (Beijing), Beijing, China, 2010. (In Chinese with English Abstract)
- Zhang, X.H.; Wu, R.H.; Wang, L.H. Research on Petrologic Character of Nephrite Jade from Baikal Lake Region in Russia. *J. Gems Gemol.* **2001**, *1*, 12–17.
- Gil, G. Petrographic and microprobe study of nephrites from Lower Silesia (SW Poland). *Geol. Q.* **2013**, *57*, 3. [[CrossRef](#)]
- Gil, G.; Barnes, J.D.; Boschi, C.; Gunia, P.; Raczyński, P.; Szakmány, G.; Bendő, Z.; Péterdi, B. Nephrite from Złoty Stok (Sudetes, SW Poland): Petrological, geochemical, and isotopic evidence for a dolomite-related origin. *Can. Mineral.* **2015**, *53*, 533–556. [[CrossRef](#)]
- Adamo, I.; Bocchio, R. Nephrite jade from Val Malenco, Italy: Review and update. *J. Gems Gemol.* **2013**, *49*, 98–106. [[CrossRef](#)]
- Zhang, Z.W.; Xu, Y.C.; Cheng, H.S.; Gan, F.X. Comparison of trace elements analysis of nephrite samples from different deposits by PIXE and ICP-AES. *X-ray Spectrom.* **2012**, *41*, 367–370. [[CrossRef](#)]
- Morin, J. The salish nephrite/jade industry: Ground stone celт production in British Columbia, Canada. *Lithic Technol.* **2016**, *41*, 39–59. [[CrossRef](#)]
- Jiang, B.H.; Bai, F.; Zhao, J.K. Mineralogical and geochemical characteristics of green nephrite from Kutcho, northern British Columbia, Canada. *Lithos* **2021**, *388*, 106030. [[CrossRef](#)]
- Leaming, S.F. *Jade in Canada*; Department of Energy, Mines and Resources: Ottawa, ON, Canada, 1978; ISBN 0660100614.
- Tan, T.L.; Ng, L.L.; Lim, L.C. Studies on nephrite and jadeite jades by Fourier transform infrared (FTIR) and Raman spectroscopic techniques. *Cosmos* **2013**, *9*, 47–56. [[CrossRef](#)]
- Liu, X.F.; Zhang, H.Q.; Liu, Y.; Zhang, Y.; Li, Z.J.; Zhang, J.H.; Zheng, F. Mineralogical Characteristics and Genesis of Green Nephrite from the World. *Rock Miner. Anal.* **2018**, *37*, 479–489. (In Chinese with English Abstract)
- Noh, J.H.; Yu, J.Y.; Choi, J.B. Genesis of nephrite and associated calc-silicate minerals in Chuncheon area. *J. Geol. Soc. Korea* **1993**, *29*, 199–224. (In Korean with English Abstract)
- Park, K.H.; Noh, J.H. Geochemical Study on the Genesis of Chuncheon Nephrite Deposit. *J. Korean Chem. Soc.* **2000**, *9*, 53–69. (In Korean with English Abstract)
- Pei, X.X. Study on the Chuncheon Nephrite Deposit, Korea—Analysis on the Mineralization and Genesis. Master’s Thesis, China University of Geosciences (Beijing), Beijing, China, 2012. (In Chinese with English Abstract)
- Pei, X.X.; Qian, Z.J.; Shi, G.H. A mineralogical study of the Chuncheon nephrite, South Korea. *Acta Petrol. Mineral.* **2011**, *90*, 89–94. (In Chinese with English Abstract)
- Yui, T.F.; Kwon, S.T. Origin of a dolomite-related jade deposit at Chuncheon, Korea. *Econ. Geol.* **2002**, *97*, 593–601. [[CrossRef](#)]
- Bai, F.; Zhao, K. Gemological and structural characteristics of nephrite from South Korea. *Acta Petrol. Mineral.* **2011**, *30*, 83–88.
- Feng, Y.H.; He, X.M.; Jin, Y.T. A new model for the formation of nephrite deposits: A case study of the Chuncheon nephrite deposit, South Korea. *Ore Geol. Rev.* **2022**, *141*, 104655.
- Hou, H.; Wang, Y.; Liu, X.F. Study of gemological characteristics of Korea nephrite jade. *Northwest. Geol.* **2010**, *43*, 147–153, (In Chinese with English Abstract)
- Kim, S.J.; Lee, D.J.; Chang, S.W. A mineralogical and gemological characterization of the Korean jade from Chuncheon, Korea. *J. Petrol. Soc. Korea* **1986**, *22*, 278–288, (In Korean with English Abstract)
- Zhao, K. Gemological and Mineralogical Study of Nephrite in South Korea. Master’s Thesis, China University of Geosciences (Beijing), Beijing, China, 2010. (In Chinese with English Abstract)
- Cho, D.L.; Suzuki, K.; Adachi, M.; Chwae, U. A preliminary CHIME age determination of monazite from metamorphic and granitic rocks in the Gyeonggi massif, Korea. *J. Earth Planet. Sci. Nagoya Univ.* **1996**, *43*, 49–65.
- Ling, X.X.; Schmädicke, E.; Wu, R.; Wang, S.; Gose, J. Composition and distinction of white nephrite from Asian deposits. *J. Mineral. Geochem.* **2013**, *190*, 49–65. [[CrossRef](#)]

25. Yang, T.T.; Wang, X.; Huang, B.; Zang, Z.Y.; Wang, J.; Yan, S.H. Origin identification of white nephrite based on terahertz time-domain spectroscopy. *Acta Petrol. Mineral.* **2020**, *39*, 314–322. (In Chinese with English Abstract)
26. Luo, Z.; Yang, M.; Shen, A.H. Origin Determination of Dolomite-Related White Nephrite through Iterative-Binary Linear Discriminant Analysis. *J. Gems Gemol.* **2015**, *51*, 300–311. [CrossRef]
27. Zhong, Q.; Liao, Z.T.; Qi, L.J.; Zhou, Z.Y. Black Nephrite Jade from Guangxi, Southern China. *J. Gems Gemol.* **2019**, *55*, 198–215. [CrossRef]
28. Bai, F.; Du, J.M.; Li, J.J.; Jiang, B.H. Mineralogy, geochemistry, and petrogenesis of green nephrite from Dahua, Guangxi, Southern China. *Ore Geol. Rev.* **2020**, *118*, 103362. [CrossRef]
29. Peng, F.; Zhao, Q.H.; Pei, L.; Wang, C.; Yin, Z.W. Study of mineralogical and spectroscopic characteristics of black nephrite from Dahua in Guangxi. *Spectrosc. Spectr. Anal.* **2017**, *37*, 2237–2241.
30. Jiang, C.; Peng, F.; Wang, W.; Yin, Z. Comparative Study on Spectroscopic Characteristics and Coloration Mechanism of Nephrite From Dahua and Luodian. *Spectrosc. Spectr. Anal.* **2021**, *41*, 1294–1299.
31. Li, N.; Bai, F.; Xu, L.L.; Che, Y.D. Geochemical characteristics and ore-forming mechanism of Luodian nephrite deposit, Southwest China and comparison with other nephrite deposits in Asia. *Ore Geol. Rev.* **2023**, *160*, 105604. [CrossRef]
32. Zhang, Y.D. Study on Geologic-Geochemical Property and Metallogenetic Regularity of Nephritic Ore in Luodian County, Guizhou Province. Master's Thesis, Guizhou University, Guiyang, China, 2015. (In Chinese with English Abstract)
33. Yang, H. A Comparative Study of Three Typical Nephrites—Taking the Examples of Guizhou Luodian Jade, Qinghai Jade and Korean Nephrite. Master's Thesis, China University of Geosciences (Beijing), Beijing, China, 2019. (In Chinese with English Abstract).
34. Bai, F.; Li, G.M.; Lei, J.; Sun, J.X. Mineralogy, geochemistry, and petrogenesis of nephrite from Panshi, Jilin, Northeast China. *Ore Geol. Rev.* **2019**, *115*, 103171. [CrossRef]
35. Zhang, C.; Yu, X.Y.; Jiang, T.L. Mineral association and graphite inclusions in nephrite jade from Liaoning, northeast China: Implications for metamorphic conditions and ore genesis. *Geosci. Front.* **2019**, *10*, 425–437. [CrossRef]
36. Wang, S.Q.; Duan, T.Y.; Zheng, Z.Z. Mineralogical and petrological characteristics of Xiuyan nephrite and its minerogenetic model. *Acta Petrol. Mineral.* **2002**, *21*, 79–90. (In Chinese with English Abstract)
37. Yu, H.Y.; Jia, Z.Y.; Lei, W. Study on Geochemical Characteristics and Influencing Factors of Rare Earth Elements in Chinese Nephrite. *Mod. Min.* **2019**, *3*, 13–17. [CrossRef]
38. Yu, H.Y.; Wang, R.C.; Guo, J.C.; Li, J.G.; Yang, X.W. Study of the minerogenetic mechanism and origin of Qinghai nephrite from Golmud, Qinghai, Northwest China. *Sci. China Earth Sci.* **2016**, *59*, 1597–1609. [CrossRef]
39. Liu, Y.; Deng, J.; Shi, G.H.; Lu, T.; He, H.Y.; Ng, Y.N.; Shen, C.H.; Yang, L.; Wang, Q. Chemical zone of nephrite in Alamas, Xinjiang, China. *Resour. Geol.* **2010**, *60*, 249–259. [CrossRef]
40. Liu, Y.; Deng, J.; Shi, G.H.; Sun, X.; Yang, L. Geochemistry and petrogenesis of placer nephrite from Hetian, Xinjiang, Northwest China. *Ore Geol. Rev.* **2011**, *41*, 122–132. [CrossRef]
41. Liu, Y.; Deng, J.; Shi, G.H.; Yui, T.F.; Zhang, G.; Abuduwayiti, M.; Yang, L.; Sun, X. Geochemistry and petrology of nephrite from Alamas, Xinjiang, NW China. *J. Asian Earth Sci.* **2011**, *42*, 440–451. [CrossRef]
42. Liu, S.W.; Lü, Y.J.; Wang, W.; Yang, P.T.; Bai, X.; Feng, Y.G. Petrogenesis of the Neoarcheangranitoid gneisses in northern Hebei Province. *Acta Petrol. Sin.* **2011**, *27*, 909–921. (In Chinese with English Abstract)
43. Chen, D.; Pan, M.; Huang, W.; Luo, W.G.; Wang, C.S. The provenance of nephrite in China based on multi-spectral imaging technology and gray-level co-occurrence matrix. *Anal. Methods* **2018**, *10*, 4053–4062. [CrossRef]
44. Liu, F.; Yu, X.Y. Classification and mineralogical characteristics of nephrite deposits in China. *Miner. Resour. Geol.* **2009**, *23*, 375–380. (In Chinese with English Abstract)
45. Gao, S.J.; Bai, F.; Heide, G. Mineralogy, geochemistry and petrogenesis of nephrite from Tieli, China. *Ore Geol. Rev.* **2019**, *107*, 155–171. [CrossRef]
46. Yin, Z.W.; Jiang, C.; Santosh, M.; Chen, Y.M.; Bao, Y.; Chen, Q.L. Nephrite jade from Guangxi Province, China. *J. Gems Gemol.* **2014**, *20*, 228–235. [CrossRef]
47. Harlow, G.; Sorensen, S.S. Jade (nephrite and jadeite) and serpentinite: Metasomatic connections. *Int. Geol. Rev.* **2005**, *47*, 113–146. [CrossRef]
48. Clayton, R.N.; Mayeda, T.K. The use of bromine pentafluoride in the extraction of oxygen from oxides and silicates for isotopic analysis. *Geochim. Cosmochim. Acta* **1963**, *27*, 43–52. [CrossRef]
49. Godfrey, J.D. The deuterium content of hydrous minerals from the east-central Sierra Nevada and Yosemite National Park. *Geochim. Cosmochim. Acta* **1962**, *26*, 1215–1245. [CrossRef]
50. Boynton, W.V. Cosmochemistry of the rare earth elements: Meteorite studies. *Dev. Geochem.* **1984**, *2*, 63–114. [CrossRef]
51. McDonough, W.; Sun, S.S.; Ringwood, A.; Jagoutz, E.; Hofmann, A. Potassium, rubidium, and cesium in the Earth and Moon and the evolution of the mantle of the Earth. *Geochim. Cosmochim. Acta* **1992**, *56*, 1001–1012. [CrossRef]
52. Graham, C.M.; Harmon, R.S.; Sheppard, S.M. Experimental hydrogen isotope studies: Hydrogen isotope exchange between amphibole and water. *Am. Mineral.* **1984**, *69*, 128–138.
53. Zheng, Y.F. Calculation of oxygen isotope fractionation in hydroxyl-bearing silicates. *Earth Planet. Sci. Lett.* **1993**, *120*, 247–263. [CrossRef]

54. Zhao, Y.H.; Yang, J.Y.; Wang, H.; Xie, Y.Q.; Li, J.X. Hydrogen and oxygen isotope distribution characteristics of geothermal water. *Prog. Geophys.* **2017**, *32*, 2415–2423. [[CrossRef](#)]
55. Zhang, Z.W.; Gan, F.X.; Cheng, H.S. PIXE analysis of nephrite minerals from different deposits. *Nucl. Instrum. Meth. B* **2011**, *269*, 460–465. [[CrossRef](#)]
56. Yu, P.H.; Ma, J.L.; Liao, J.B.; Li, Z.Y.; Di, J. Geochemistry and paleoenvironment significance of Lulehe Formation Xiaganchaigou Formation located in the north area of Qaidam Basin. *Arid Land Geogr.* **2020**, *43*, 679–686. (In Chinese with English Abstract)
57. Imeokparia, E.G. Ba/Rb and Rb/Sr ratios as indicators of magmatic fractionation, postmagmatic alteration and mineralization Afu Younger Granite Complex, Northern Nigeria. *Geochem. J.* **1981**, *15*, 209–219. [[CrossRef](#)]
58. Tang, J.; Zheng, Y.F.; Wu, Y.B.; Zha, X.P.; Zhou, J.B. Zircon U-Pb ages and oxygen isotopes of high-grade metamorphic rocks in the eastern part of the Shandong Peninsula. *Acta Petrol. Sin.* **2004**, *20*, 1039–1062. (In Chinese with English Abstract)
59. Wang, Y. Metamorphic and Deformation Characteristics in Northwest Yunnan Province of Nu River Chongshan Group Metamorphic Complex. Master’s Thesis, Guilin University of Technology, Guilin, China, 2018. (In Chinese with English Abstract)

**Disclaimer/Publisher’s Note:** The statements, opinions and data contained in all publications are solely those of the individual author(s) and contributor(s) and not of MDPI and/or the editor(s). MDPI and/or the editor(s) disclaim responsibility for any injury to people or property resulting from any ideas, methods, instructions or products referred to in the content.